Millimeter-wave Field Experiments with Many Antenna Configurations for Indoor Multipath Environments

Marcus Comiter[1], Michael Crouse[1], H. T. Kung[1], Jenn-Hwan Tarng[2], Zuo-Min Tsai[3], Wei-Ting Wu[2], Ta-Sung Lee[2], M. C. Frank Chang[2], and Yen-Cheng Kuan[2]

[1]Harvard University, [2]National Chiao Tung University, [3]National Chung Cheng University

Abstract—Next-generation wireless networks, such as 5G networks, will use millimeter waves (mmWaves) operating at 28 GHz, 38 GHz, 60 GHz, or higher frequencies to deliver unprecedentedly high data rates, e.g., 10 gigabits per second. Due to high attenuation at this higher frequency, use of directional antennas is commonly suggested for mmWave communication. It is therefore important to study how different antenna configurations at the transmitter and receiver effect received power and data throughput. In this paper, we describe field experiments with mmWave antennas for indoor multipath environments and report measurement results on a multitude of antenna configurations. Specifically, we examine four different mmWave systems, operating at two different frequencies (38 and 60 GHz), using a number of different antennas (horn antennas, omnidirectional antennas, and phase arrays). For each system, we systematically collect performance measurements (e.g., received power), and use these to examine the effects of beam misalignment on signal quality, the presence of multipath effects, and susceptibility to blockage. We capture interesting phenomena, including a multipath scenario in which a single receiver antenna can receive two copies of signals transmitted from the same transmitter antenna over multiple paths. From these field experiments, we discuss lessons learned and draw several conclusions, and their applicability to the design of future mmWave networks.

Keywords—millimeter waves, antenna patterns, 5G, 802.11ad, power-delay measurements, multipath, field experiments.

I. INTRODUCTION

Next-generation wireless networks, such as 5G networks, will use millimeter waves (mmWaves) operating at 28 GHz, 38 GHz, 60 GHz, or higher frequencies to deliver unprecedentedly high data rates, e.g., 10 gigabits per second. Due to high attenuation at this higher frequency, mmWave communication calls for the use of directional antennas. Experimental investigations of 60 GHz spatial and temporal characteristics have confirmed that at such high frequencies, propagation is quasi-optical in nature and the ray tracing technique based on geometric optical approximation can be applied [1], [2] . It has also been found that reflected waves needed to be considered, especially in non-LOS (Line-Of-Sight) situations. Measurements covering a wide range mmWave bands such as 28, 38, 60 and 73 GHz for access, backhaul, peer-to-peer, and vehicle-to-vehicle scenarios have been illustrated and analyzed [3]. 60 GHz and 28 GHz radio propagation measurement campaigns have been also executed in indoor office environments to explore detailed multipath cluster characteristics [4], [5]. It has been found that mm-wave radio channels exhibit simple multipath constellation and significant angular sparsity [5]. Recently, multi-frequency mmWave massive MIMO radio channel measurements, characterization, and models have been conducted. In [6], measurements of massive channels at 11, 16, 28 and 38 GHz bands indoor environments using a large virtual uniform rectangular array are illustrated. New massive MIMO properties such as spherical wavefront, cluster birth-death, and the non-stationarity over the array have been explored by using the spatio-temporal multipath-component variations over the array. In [7], a measurement campaign of 26 GHz massive MIMO is conducted using a virtual 64-element linear/planar array or a virtual 128-element planar array. Data of path loss, shadow fading, and delay spread are extracted or estimated.

This directionality of mmWaves poses new challenges to systems. Not only does it require new service paradigms, such as the ability for the transmitter (Tx) and receiver (Rx) to align their beams, but the paradigm is also catalyzing the introduction of not one but many different types of antennas. As such, mmWave systems may use horn antennas, pseudo-omni-directional antennas, phase arrays, or a combination of all three, operating on equipment built by different vendors, each with their own characteristics. However, system effects of various mmWave antenna configurations are not well studied, and have not been validated across real-world mmWave platforms/systems. It is urgent to address these challenges for the development of service stacks to power emerging networks such as 5G mobile networks and 802.11ad networks.

In this paper, we examine the behavior of mmWave antennas in real-world environments using several systems in the field, motivated by the fact that gaining physical insights into the actual systems should allow for improved design of future networks. In these field experiments we measure system performance (e.g., received power) under a variety of antenna configurations. For example, the transmitter and receiver use horn and omni-directional antennas of certain types, respectively. To cross validate our measurement results, we use multiple mmWave platforms from different vendors. Specifically, we experiment with four different systems, operating at two different frequencies (38 and 60 GHz), using a number of different antennas (horn antennas, omni-directional antennas, and phase arrays), in indoor multipath environments. For each system, we systematically collect measurements, and use these to examine the effects of beam misalignment on signal quality, the presence of multipath effects, and susceptibility to blockage. Our paper explores the effects of transmitter and receiver antenna patterns on end-to-end system performance. Both patterns play a role in spatial filtering mechanism, which may filter out specific AoD and AoA paths. To optimize the system performance, transmitter and receiver antenna patterns are required to match with radio channel spatial responses.

Following the presentation of the experiments and results, we discuss insights learned and takeaways, and their applicability to the design of mmWave networks that will be useful to the community-at-large. We find that multipath is

significant and relevant in all systems, and discuss the tolerance of alignment error. In addition, we identify an interesting phenomenon, namely a scenario when the transmitter and the receiver are not aligned with one another, the receiver with a wide beam antenna can still receive the line-of-sight (LOS) signal and a non-line-of-sight (NLOS) signal emitted from a side lobe and the main lobe of the transmitter antenna, respectively. This scenario implies the possibility of using multipath signals and side lobes to sustain data links under intermittent blockage in mmWave networks. This suggests a potential asymmetric antenna pattern design strategy for transmitter and receiver, which is not common in the current wireless networks (below 6 GHz).

In Sections II and III, four radio sounding systems and measurement sites are introduced, respectively. In Section IV, the experiments performed and present results are discussed. In Section V, insights learned and takeaways are presented. Conclusion is drawn in Section VI

II. RADIO SOUNDING SYSTEMS

In this section, we describe the four mmWave radio sounding systems used in our experiments. These equipment systems are manufactured by three vendors, operate over two frequencies, and use two families of antennas, namely end-fire (highly directional) antennas and omni-directional antennas. Comparing the performance of the systems from different vendors provides an important view on the state of mmWave equipment development and performance across manufacturers. The field measurmeents with asymmetric transmitting and receiving antenna patterns is done to explore the coupling effects among antenna patterns and the multipath propagation from a single transmitter to a single receiver.

A. Equipment System 1: Rohde & Schwarz 38 GHz Sounder with Horn to Custom Omni-directional Antenna

The first equipment system is a Rohde & Schwarz mmWave sounding system operating at 38 GHz. The system uses a horn antenna with a 14 degree half power beam width (HPBW) as the transmitter antenna, and a custom-made omni-directional antenna as the receiver antenna. The gain of the horn antenna is 25 dBi. Both the transmitter antenna and the receiver antenna are mounted on a custom gimbal, which rotates the antenna in the left-right directions with a minimum step size of 0.010 degrees. Additionally, the transmitting and receiving antennas are mounted on a one-meter track that can move the antennas laterally (closer and farther from one another) with a minimum step size of 0.01m.

B. Equipment System 2: Rohde & Schwarz 60 GHz Sounder with Horn to Custom Omni-directional Antenna

The second equipment system is the same Rohde & Schwarz mmWave sounding system, but operates at 60 GHz. The system uses a horn antenna with an 11 degree HPBW as the transmitting antenna, and a wide beam antenna with an 80 degree half power beamwidth as the receiving antenna. Both the transmitter antenna and the receiver antenna are mounted on a custom gimbal, which rotates the antenna in the left-right directions with a minimum step size of 0.010 degrees. Additionally, the transmitting and receiving antennas are mounted on a one-meter track that can move the antennas

laterally (closer and farther from one another) with a minimum step size of 0.01m.

C. Equipment System 3: Keysight 60 GHz sounder with Horn to Horn Antennas

The third equipment system is a Keysight mmWave sounding system operating at 60 GHz. The system uses a horn antenna with an 11 degree HPBW as the transmitter antenna, and a horn antenna with an 11 degree half power beam width as the receiver antenna. Both the transmitting and the receiving antennas are mounted on a custom gimbal, which can rotate the antenna in the left-right directions with a minimum step size of 0.129 degrees. For all experiments with this system, the transmitter and receiver nodes are mounted on tripods that are laser aligned to grid markings carefully placed on the floor.

D. Equipment System 4: Commercialized 60 GHz USB Dongles

The fourth equipment system is a commercialized UE system operating at 60 GHz. The system uses a 2Tx2R MIMO antenna with a 60 degree HPBW as the transmitter antenna and the receiver antenna. The receiving and transmitting nodes connect to a commercial laptop via a USB 3 connection. Both the transmitting and the receiving antennas are mounted on a custom gimbal, which can rotate the antenna in the left-right directions with a minimum step size of 0.129 degrees. For all experiments with this system, the transmitter and receiver nodes are mounted on tripods that are laser aligned to grid markings carefully placed on the floor.

III. TEST SITES

In this section, we describe two different test sites chosen for our field experiments. These test sites represent realistic indoor deployment environments in which mmWave systems, such as 5G networks and 802.11ad networks, are expected to operate. The test sites span different operating characteristics, including space, proximity to objects and walls that can potentially cause interference or multipath effects, and the presence or absence of reflecting material. Comparing the performance of systems between the two test sites offers important insights into the behavior of mmWave systems in different environments.

A. Free Space Lobby

The first test site is a large lobby in an academic building. This room has a glass wall on one side, and a drywall on the opposite side, and a large, open space whose center point was approximately 20 feet from either side. Due to the large size of the test site, experiments in this environment allow for devices to be placed far enough away all walls in order to reduce their impact on measurements taken.

B. Small Office Room

The second test site is a small room in an academic office building. This room has walls made of drywall as well as several windows covered with reflective metallic paper. This room is significantly smaller than the first test site. Therefore, it is relatively more difficult to stop potential multipath effects due to close proximity of walls and transmitter/receiver nodes.

IV. Experiments

In the following sections, we describe four experiments. Experiment 1 studies the effect of misalignments between a transmitting node and a receiving node. Experiment 2 studies and compares the multipath behavior of the same system operating at different frequencies, 38 GHz and 60 GHz. Experiment 3 studies the multipath behavior of a 60 GHz system. Experiment 4 studies the alignment of mmWave UE equipment with a large antenna beamwidth. We first describe the experimental framework used across all experiments. Following this, for each experiment, we present the experimental plan, and present results. In Section V, we present insights learned from these experiments.

A. Experimental Framework

For all experiments and figures, we use the convention that the direction of 90 degrees is aligned with the direction of the line-of-sight path. Each measurement of every experiment is performed a minimum of two times (i.e., two samples are taken). Generally, results are found to agree across these two measurements.

B. Experiment 1: Rx and Tx Alignment Sensitivity

Experiment 1 studies the effect of misalignments between a transmitting node and a receiving node using Equipment System 3, the Keysight 60 GHz Horn to Horn system. The motivation behind this experiment is the fact that mmWave transmitters and receivers will need to align their beams through the beam steering process in order to communicate. As such, it is important to understand how misalignments will impact signal quality. Experiment 1 is performed in Test Site 1 (free space lobby).
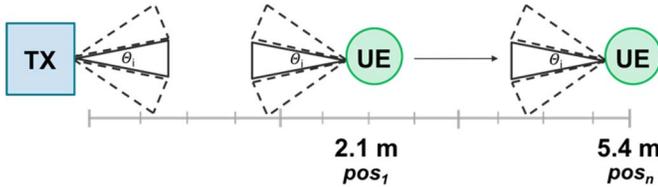

Fig. 1. The experimental setup of Experiment 1. The receiver node is positioned at set distances (2.1 m, 3.7 m, 5.4 m) from the transmitter node. The transmitter and receiver nodes are rotated.

The experimental plan, as shown in Figure 1, is as follows:

1) Position the receiver node at set distances (2.1 m, 3.7 m, 5.4 m) from the transmitter node.
2) For each receiver node location, rotate the receiver in 5 degree intervals, from 0 degrees to 180 degrees, using the gimbal.
3) For each receiver location and angle, rotate the transmitter node in 5 degree intervals, from 0 degrees to 180 degrees.
4) For each position and configuration, measure received packet power.

We note that it is important to rotate both the transmitter node and the receiver node in order to capture all receiver-transmitter antenna configuration (angle of departure, angle of arrival) pairs. To understand this, consider the scenario in which only the receiver is rotated and the transmitter remains fully static. This is shown on the left-hand side of Figure 2. If only the receiver node is rotated, a number of configurations between the receiver and transmitter nodes are not tested. For example, configurations in which the transmitter and receiver are nearly or completely parallel with one another do not occur when only the transmitter is rotated. However, these additional configurations are tested when both the receiver and transmitter are rotated, as shown on the right-hand side of Figure 2.
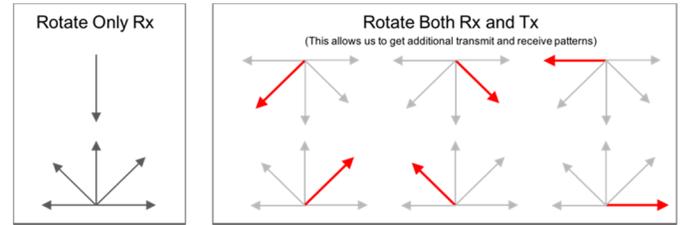

Fig. 2. It is important to rotate both the receiver and transmitter antennas. When only the receiver is rotated (left), there are a number of receiver and transmitter configurations that are not captured, such as the receiver and transmitter being parallel to one another. However, when both the receiver and transmitter are rotated, these additional configurations can be measured.
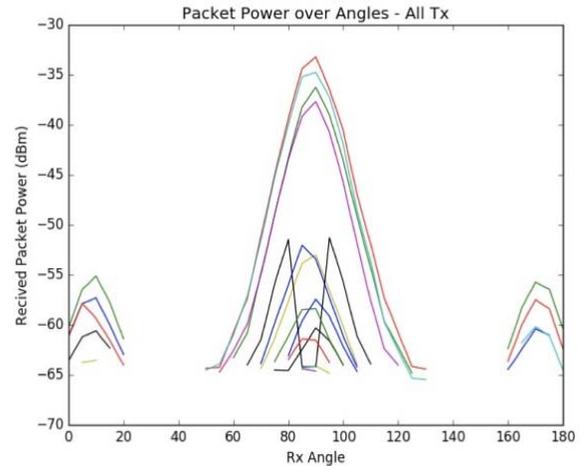

Fig. 3. The experimental results of Experiment 1 showing the effect of antenna misalignment on received packet power for a single fixed distance (2.1 m) between the receiver and transmitter. The receiver angle is shown on the x-axis, and received packet power (in dBm) on the y-axis. Each line corresponds to a different transmitter alignment.

We measure the received packet power at each receiver-transmitter antenna configuration at each position. We first consider the impact of the receiver-transmitter configuration for a fixed location. These results are shown in Figure 3. In this figure, the receiver angle is shown on the x-axis, and each line corresponds to a different transmitter angle. We find that received packet power falls off quickly past the optimal alignment.
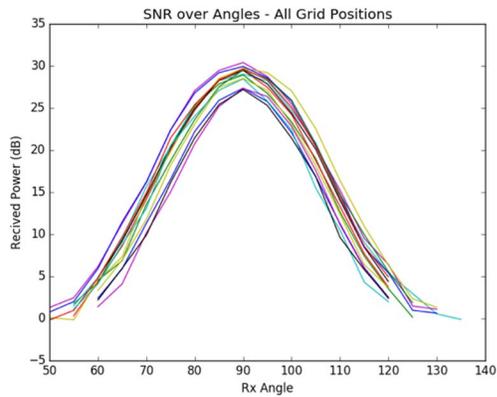
Fig. 4. The effects of distance on received packet power for Experiment 1. In this graph, the transmitter is not rotated in order to isolate the effects of changing distance. Each line corresponds to a different distance between the transmitter and receiver. The lines with the higher received packet power correspond to closer distances between the transmitter and receiver.

Next, we examine the results of antenna alignment as distances changes. Figure 4 shows the effects of changing distance between transmitter and receiver antennas on received packet power, where each line corresponds to a different distance between the transmitter and receiver. The lines with higher received packet power correspond to closer distances between the transmitter and receiver. There are two notes of interest. First, we find that increasing distance reduces received packet power, but not as significantly as the reduction in received packet power due to antenna misalignment. The reduction in received packet power from the point closest to the transmitter (2.1 m) to the point farthest from the receiver (5.4 m) is only 5 dB. Second, we find that the received packet power falls off quicker as distance between the receiver and transmitter antennas increases. This is expected, as at further distances, the effects of misalignments are magnified. As a result, there is less tolerance, and therefore a need for higher beam alignment accuracy, when the transmitter and receiver are farther apart from one another.

C. Experiment 2: Number of Multipath Bounces

This experiment compares the multipath behavior of the same system operating at 38 GHz and 60 GHz, and examines how many multipath bounces are detectable/usable by the system. Experiment 2 uses Equipment System 1 (Rohde & Schwarz 38 GHz Horn to Omni) and System 2 (Rohde & Schwarz 60 GHz Horn to Omni). Experiment 2 is performed at Test Site 2 (small office room).

This motivation behind this experiment is to study the behavior of multipath at different frequencies that are expected to be used by mmWave systems. The effects of multipath behavior in mmWave systems are of interest to the community but not well understood. Unlike in lower frequencies, the multipath behavior of mmWave frequencies will be characterized by a small number of bounces, which may or may not be useful as an additional avenue for signal delivery. The goals of this experiment are to understand how multipath is similar/different in the 38 GHz and 60 GHz frequency bands, and to understand how strong the multipath effects are (e.g., how

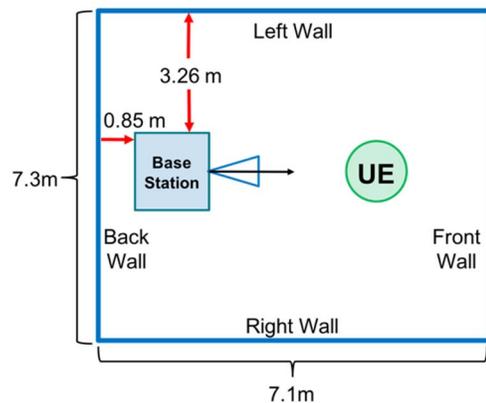many bounces are sufficiently strong such that they can be detected by the system).

Fig. 5. The experimental setup of Experiment 2, which studies the multipath behavior of a mmWave system operating at two frequencies, 38 GHz and 60 GHz.
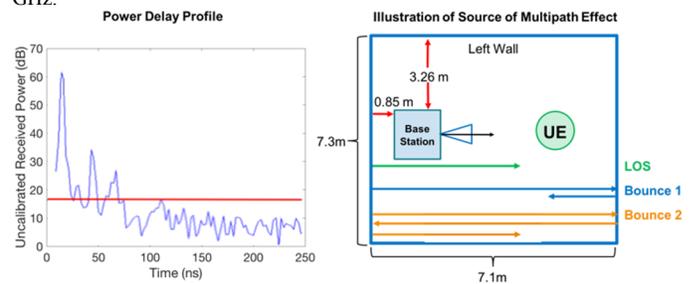

Fig. 6. Results for Experiment 2 at 38 GHz. A power delay profile (PDP) is shown in left figure, and shows that the system can detect three paths (LOS path, a bounce-once path due to refection by the front wall, and a bounce-twice path due to reflection by the front wall, then by the back wall). These multiple sources of multipath bounces are illustrated in the right figure.

The experimental plan, as shown in Figure 5, is as follows:

1) Position the receiver node at a set distance (2.1 m) from the transmitter node, such that the transmitter node is directly in front of the back wall of the room, and the receiver node is in front of the front wall of the room.
2) Transmit from the horn transmitter antenna to the omni receiver antenna.
3) Measure a power delay profile over a set time period.
4) Repeat the experiment at 60 GHz

We first examine the results of Experiment 2 for a single frequency band. This allows us to identify how many multipath bounces can be detected by the system. The results of Experiment 2 for the 38 GHz system are shown in Figure 6. As the figure shows, three paths are sufficiently strong such that they can be identified and used by the system. These three paths correspond to the line-of-sight path, a single bounce path due to refection by the front wall, and a double bounce path due to reflection by the front wall, then by the back wall. Note that via its omni antenna, the UE can receive signal from the Tx and those bounced from the walls. The measured propagation time of each path is aligned with the theoretical result according to the corresponding geometrical path length divided by speed of light. Next, we compare the results of the system operating at 38

GHz and 60 GHz. The results are shown in Figure 7. We find that both systems show the same behavior, both identifying three paths.
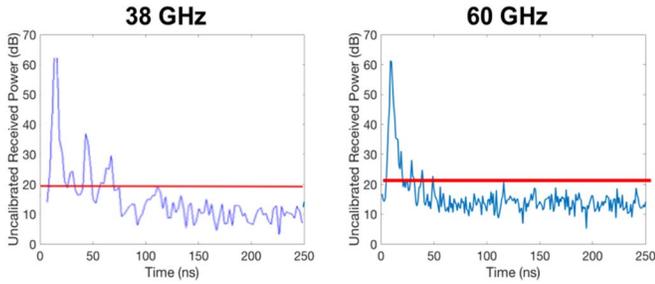

Fig. 7. Comparison of multipath effects at 38 GHz (left) and 60 GHz (right). We find that at both frequencies, three paths are detected by the system.
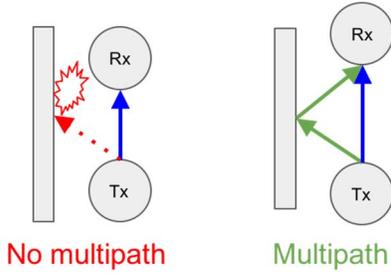

Fig. 8. The experimental setup of Experiment 3. When the setup shown on the left-hand side (pointing the receiver and transmitter at one another), no parallel signal path was detected. However, when pointing the transmitter at the wall and the receiver at the transmitter, this phenomenon was observed.

D. Experiment 3: Simultaneous Receiving of Parallel Signals from Single Transmitter

This experiment studies the multipath behavior of a 60 GHz system, and demonstrates the phenomenon in which the same receiver antenna can receive two parallel signals transmitted from the same transmitter antenna. Experiment 3 is performed with Equipment System 3 (Keysight 60 GHz Horn to Horn). The experiment is performed in Test Site 1 (free space lobby).

Hoping to capture multipath effects, we positioned the transmitter and receiver close to the wall, aimed the transmitter and receiver at one another. However, no multipath effects were observed. This is illustrated in Figure 8 on the left-hand side. However, we then aimed the transmitter at the wall and the receiver at the transmitter, such that the line-of-sight beam would be from the side lobe, and the direct path would be from the multipath, and in this case saw multipath effects. This is illustrated in Figure 8 on the right-hand side.

The experimental plan, as shown in Figure 8, is as follows:

1) Position the receiver node and transmitter node 1m from a wall.
2) Aim both the receiver node and transmitter node at the same spot on the wall, and transmit a signal from the transmitter to the receiver node. Record a power delay profile.
3) Aim the transmitter directly at the receiver node. Aim the receiver node at the wall. Transmit a signal from the transmitter. Record a power delay profile.
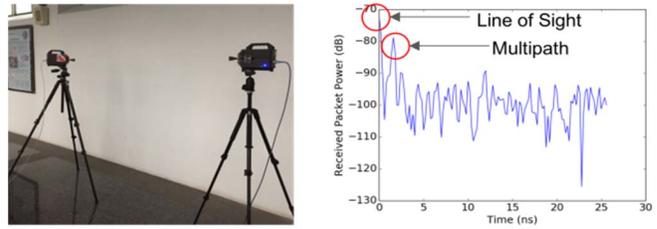

Fig. 9. Multipath bounces for Experiment 3. We see peaks from both the line-of-sight beam and the beam from the multipath effect.
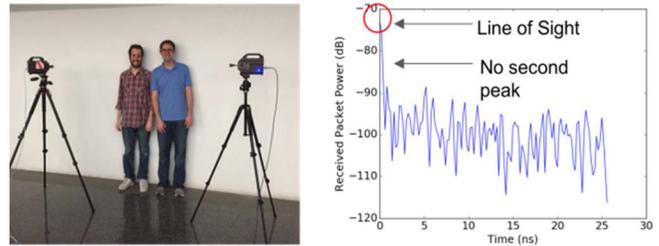

Fig. 10. Multipath effects of Experiment 3 disappear when absorbers are present.

Figure 9 shows two multipath bounces are sufficiently strong such that they can be identified and used by the system. These bounces correspond to the line-of-sight from the side lobe of the transmitter antenna, and are reflected by the wall to the receiver. The measured propagation time of each path is confirmed by the calculation reflecting the corresponding geometrical path length divided by speed of light.

Next, the presence of multipath effects due to physical boundaries is verified by placing two mmWave absorbing blockers on the wall. If there is indeed a significant bounce due to the side-lobe-directed wave reflected by the wall, the addition of these absorbers should make the reflected wave disappear. Figure 10 shows the setup with absorbers and power delay profile for this additional experiment. As this shows, the bounce due to the wall reflection does in fact disappear, which means that the coupling among antenna patterns and propagation plays an important role in determining number of received parallel signals from a single transmitter.

E. Experiment 4: mmWave UE Alignment Sensitivity

This experiment studies the alignment of mmWave UE equipment with a large HPBW antenna. Experiment 4 is performed with Equipment System 4 (Commercialized 60 GHz UE) in test site 1 (free space lobby). The modulation coding scheme is set to be Binary Phase Shift Keying (BPSK) for all measurements.

This experiment is to examine the effects of misalignment on actual measured data throughput, rather than a characteristic of signal quality such as received packet power.

The experimental plan, as shown in Figure 1, is as follows:

1) Position the receiver node at set distances (2.1 m, 3.7 m, 5.4 m) from the transmitter node.
2) For each receiver location, rotate it in 5 degree intervals, from 0 to 180 degrees, using the gimbal.

3) For each Rx location and angle, rotate the transmitter node in 5 degree intervals, from 0 to 180 degrees.
4) For each position/configuration, measure throughput.

Figure 11 shows that there exists a safe window of misalignments such that as long as the alignment is sufficiently close, there is no noticeable effect on data throughput. However, outside of this window, data throughput drops significantly. Further, we note that as the distance between the transmitter and receiver increases, the window of acceptable misalignment grows smaller. This is explained by the fact that as the distance between the receiver and transmitter increases, the effects of antenna misalignment are magnified.
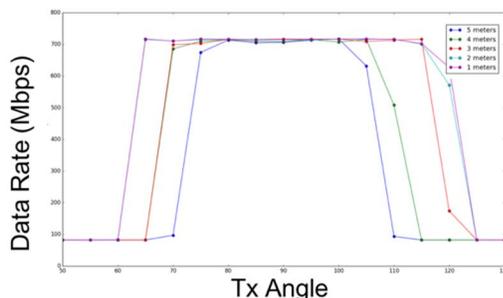

Fig. 11. Experimental results of Experiment 4. We find that as the distance between the transmitter and receiver increases, the window at which usable data rates can be achieved decreases. Maximum data rates are capped by the modulation scheme used in our experiment setups.

V. INSIGHTS LEARNED AND TAKEAWAYS

In this section, we discuss insights learned from the results of the experiments performed in the previous section.

A. Multipath is Significant

The first insight is that multipath effects are significant for mmWave systems. Before running these experiments, we were unsure as to the presence/usability of multipath in mmWave systems. Specifically, we wondered if the multipath effects would not be strong enough to support resilience in data transmission. However, as shown by Experiments 2 and 3, observable multipath effects are in fact significant, and are not limited to just one bounce.

Beyond traditional multipath effects, we also discover a new effect that both the main and side lobe of the transmitter horn antenna can introduce a parallel channel over which the same signal can be sent. More specifically, although the transmitter and receiver each only use one antenna, leveraging the multipath environment, multiple signal paths can be used such that the receiver with a wide beam antenna can receive multiple copies of the same signal emitted by the transmitter antenna. Being able to receive the same signal from multiple paths will lend itself to improved reliability in communication, especially where intermittent blockages could be frequent. These multipath effects, coupled with omni-directional antennas at the receiver, can be an important mechanism for making indoor mmWave systems more robust.

B. Omni-directional UEs are Relevant

Our initial belief was that high frequency channels, particularly in indoor environments, would require the use of highly directional antennas on both sides of the channel (i.e., on both the base stations and UEs) in order to compensate for the increased attenuation. However, after working with the 802.11ad devices (e.g., Equipment System 4 for Experiment 4), we found that the communication distance was greater than expected even with wider beam antennas (60° HPBW).

We find that the devices truly do achieve an impressively high data rate (approximately 1 Gbps) at 1 meter distance between the transmitter and receiver. Further, the devices are able to achieve greater than 300 Mbps data rates at distances of approximately 15 meters in an indoor environment. Although more complex multipath behavior could cause interference, such as two-ray effects, this study is an important first step in showing that wider beam antennas on user endpoints is possible.

C. Tolerance for Misalignment Exists

An important aspect of mmWave systems is the need for transmitter and receiver beams to align their antennas with one another. In all experiments, we find that there is a reasonable amount of tolerance to antenna misalignment. Given this tolerance to some misalignment, these experiments show that beam alignment procedures need not be perfect.

VI. CONCLUSION

We have measured received power and achieved throughput as a function of transmitter and receiver antenna configurations using multiple mmWave equipment systems spanning multiple vendors, antenna types, and frequencies. We study the effects of antenna misalignment and multipath in real-world indoor environments. We have found that the measurement results and behavior of the systems are largely reliable and consistent across equipment systems and frequencies. We conclude that multipath effects are significant and can be exploited, mmWave UE can achieve high data rates in indoor environments, and significant tolerance exists for antenna misalignment.

VII. ACKNOWLEDGMENTS

REFERENCES

[1] Hao Xu, Vikas Kukshya, and T.S. Rappaport, "Spatial and temporal characteristics of 60-GHz indoor channels," IEEE J. Select. Areas Commun., vol. 20, no. 3, pp.620-630, April 2002.

[2] A. Maltsev, R. maslennikov, A. Sevastyanov, A. Khoryaev, and A. Lomayev, "Experimental investigations of 60 GHz WLAN systems in office environment," IEEE J. Select. Areas Commun., vol. 27, no. 8, pp.1488-1499, Oct. 2009.

[3] T. S. Rappaport, G. R. MacCartney, M. K. Samimi and S. Sun, "Wideband Millimeter-Wave Propagation Measurements and Channel Models for Future Wireless Communication System Design," in *IEEE Transactions on Communications*, vol. 63, no. 9, pp. 3029-3056, Sept. 2015.

[4] X. Wu *et al*., "60-GHz Millimeter-Wave Channel Measurements and Modeling for Indoor Office Environments," in *IEEE Transactions on Antennas and Propagation*, vol. 65, no. 4, pp. 1912-1924, April 2017.

[5] X. Yin, C. Ling and M. D. Kim, "Experimental Multipath-Cluster Characteristics of 28-GHz Propagation Channel," in *IEEE Access*, vol. 3, no. , pp. 3138-3150, 2015.

[6] J. Huang, C. X. Wang, R. Feng, J. Sun, W. Zhang and Y. Yang, "Multi-Frequency mmWave Massive MIMO Channel Measurements and Characterization for 5G Wireless Communication Systems," in *IEEE Journal on Selected Areas in Communications*, vol. 35, no. 7, pp. 1591-1605, July 2017.

[7] B. Ai *et al*., "On Indoor Millimeter Wave Massive MIMO Channels: Measurement and Simulation," in *IEEE Journal on Selected Areas in Communications*, vol. 35, no. 7, pp. 1678-1690, July 2017.